Article

DNA methylation on N6-adenine regulates the hyphal development during dimorphism in the early-diverging fungus *Mucor lusitanicus*

Macario Osorio-Concepción [1], Carlos Lax [1], Eusebio Navarro [1], Francisco E. Nicolás [1,*] and Victoriano Garre [1,*]

[1] Departamento de Genética y Microbiología, Facultad de Biología, Universidad de Murcia; macario.osorio@um.es, carlos.lax@um.es, sebi@um.es, fnicolas@um.es, vgarre@um.es.
* Correspondence: vgarre@um.es, fnicolas@um.es

Abstract: The epigenetic modifications control the pathogenicity of human pathogenic fungi, which have been poorly studied in Mucorales; causative agents of mucormycosis. This order belongs to a group referred to as early-diverging fungi that are characterized by high levels of N6-methyldeoxyadenine (6mA) in their genome with dense 6mA clusters associated with actively expressed genes. AlkB enzymes can act as demethylases of 6mA in DNA, with the most remarkable eukaryotic examples being mammalian ALKBH1 and *Caenorhabditis elegans* NMAD-1. *Mucor lusitanicus* (formerly *M. circinelloides* f. *lusitanicus*) genome contains one gene, *dmt1*, and two genes, *dmt2* and *dmt3*, encoding proteins homologs to *C. elegans* NMAD-1 and ALKBH1, respectively. The function of the three genes was analyzed by the generation of single and double deletion mutants for each gene. Multiple processes were studied in the mutants, but defects were only found in single and double deletion mutants for *dmt1*. In contrast to the wild-type strain, *dmt1* mutants showed an increase of 6mA levels during the dimorphic transition, suggesting that 6mA regulates dimorphism in *M. lusitanicus*. Furthermore, the spores of *dmt1* mutants challenged with macrophages underwent a reduction of polar growth, suggesting that 6mA also has a role during the spore-macrophage interaction that could be important in the infection process.

Keywords: Mucormycosis; AlkB; demethylase, virulence, dimorphism, protein kinase A, hyphae development, Mucor.

1. Introduction

Mucormycosis is an invasive and emerging infection produced by opportunistic fungi of the order Mucorales [1,2]. The infection is characterized by blood vessel invasion and thrombosis formation, concluding in tissue necrosis facilitating the fungal spreading [3]. Furthermore to patients with pathologies, such as diabetes and impaired immune system, healthy individuals are also the most at risk for fungal infection (Ibrahim, 2011). Mucormycosis has been increasingly described in patients COVID-19 associated with uncontrolled diabetes and steroid treatment [4,5]. This concerning scenario caused by the high mortality rates of mucormycosis (up to 90%) has provoked an urgent need to study this lethal infection [6]. Therefore, identifying essential components to the development of mucoralean fungi could contribute to the design of new specific and effective antifungal therapies. In study of the mucormycosis-causing fungi, *M. lusitanicus* (formerly *M. circinelloides* f. *lusitanicus*) [7] has become an excellent genetic model to elucidate the molecular mechanisms of the infection process in the host. The growing development of new molecular and genetic strategies to manipulates the *M. lusitanicus* genome has enabled the discovery of diverse virulence processes important for establishing infection, such as iron assimilation, dimorphism, and RNA interference mechanism (RNAi) [8,9]. The dimorphism of some Mucorales species consists of the ability to change the growth form between yeast and hyphae, a process regulated by environmental conditions [9,10]. In

 doi:10.20944/preprints202107.0525.v1

aerobic conditions, *M. lusitanicus* exhibits filamentous growth, while in an anaerobic environment grows exclusively as yeast [11]. Recent studies revealed a connection between the calcineurin pathway, dimorphism, and virulence of *M. lusitanicus*. Calcineurin is a heterodimeric Ca^{2+}/calmodulin-dependent phosphatase constituted by a regulatory (CnbR) and a catalytic subunit (CnaA), regulating the activity of transcription factors through dephosphorylation [12]. The CnbR and CnaA deletion from Calcineurin affect the considerably dimorphic transition [13,14]. Strain blocked in filamentous growth showing high virulence, while strains that exclusively grow as yeast are less virulent [13,14]. Other proteins, such as cAMP-dependent protein kinase A (PKA), also mediate the dimorphism and virulence of *M. lusitanicus* [15,16].

However, the pathogenicity mechanisms used by *Mucorales* to invade the host and develop the infection have not been completely characterized. In this context, understanding how epigenetic modifications in nucleic acids and proteins influence essential functions in diverse biological processes could be powerful knowledge to obtain effective treatments. For instance, in the human pathogen *Candida albicans*, epigenetic modifications control diverse virulence factors, including antifungal resistance, host biofilm formation, and switch from yeast to hyphae [17–19]. DNA methylation is one of these covalent modifications and can be incorporated in DNA as a result of lesions induced by alkylating agents or catalyzed by specific methylases proteins. This epigenetic mark is associated with diverse cell processes in prokaryotes and eukaryotes [20,21]. C5-methylcytosine (5mC) is the most frequent form of DNA methylation in eucaryotes organisms, which involves epigenetic memory maintenance, regulation of gene expression, transposon inactivation, and genomic imprinting [21,22]. Another form of DNA methylation is N6-methyldeoxyadenine (6mA), initially found in prokaryotic organisms, which has been recently identified in several eukaryotes being involved in processes such as regulation of gene expression and transposons, tumorigenesis, stem cell differentiation, and mismatch repair [23,24]. High levels of 6mA have been detected in early diverging fungi, including Mucorales, suggesting that it plays important role in the biology of these fungi. [25]. Genome analysis of several fungi species revealed early fungi contain up to 2.8% of methylated adenines, contrary to the tested higher fungi and other eucaryotes containing 6mA between 0.048 and 0.21%, respectively [25]. The analysis also revealed that 6mA occurs in the ApT dinucleotide of both DNA strands. Most of the 6mA marks are concentrated in methylated adenine clusters (MACS), which are localized around the promoter regions of transcriptionally active genes indicating that they could relevant for gene expression regulation [25]. In eukaryotes with elevated 6mA levels in DNA such as *Chlamydomonas reinhardtii* and the ciliates *Oxytrichia trifallax* and *Tetrahymena thermophila*, 6mA distribution also prevails in the ApT sites close to the transcription start sites of active genes [26–28]. The recent discovery of proteins responsible for removing methyl groups of 6mA indicates that DNA adenine methylation is a dynamic modification [29]. The demethylation of DNA adenine is accomplished by the activity of 2-oxoglutarate/Fe (II)-dependent dioxygenases enzymes (AlkB), which are conserved from prokaryotes to eukaryotes [30,31]. Bacterial genomes contain between one and three AlkB enzymes important to restore DNA lesions, such as N1-Methyladenine (1mA), N3-methylcytosine (3mC), N3-methylthymine (3mT), induced by alkylating agents [32–34]. Notably, a variety species of eukaryotes, including mammals, yeasts, and plants, contain bacterial AlkB homologs (ALKBH), with the conserved AlkB domain indicating potential functions in various cell processes [35–37]. Humans and mice contain nine ALKBH, designated as AlKBH1-8 and FTO (Fat mass and obesity-associated), localized in different cell compartments [35,38,39]. Like bacterial AlkB enzymes, each member of the ALKBH family preferentially recognizes and demethylates a type of methylation from DNA or RNA [35]. In mammals, AlKBH proteins appear to be associated with genomic stability maintenance, methylated nucleotide repair, and inhibition of tumor development [40,41]. In recent years, the biological function of DNA and RNA demethylation mediated by ALKBH1 has been extensively studied [42]. It has been found that human ALKBH1 (hALKBH1) shows preference towards the substrates 5-methylcytosine (5mC), 3-methylcytidine (3mC), 6mA, 1-methyladenosine (1mA),

Preprints (www.preprints.org) | NOT PEER-REVIEWED | Posted: 23 July 2021 doi:10.20944/preprints202107.0525.v1

suggesting a hALKBH1 role in gene regulation, transduction, and mitochondrial activity [43]. The hALKBH1 overexpression and the consequent decrease of 6mA levels promote the proliferation, migration, and invasion of cancer cells, indicating 6mA functions in the tumorigenesis inhibition [44,45]. In mice, the ALKBH1 absence causes alterations in the development and neuronal differentiation [46,47]. In *Caenorhabditis elegans*, from five ALKB proteins found, only one of them shows demethylase activity to 6mA from DNA. The deletion of N6-methyl adenine demethylase 1 (*nmad*-1) results in mutants worms sterile and present a high accumulation of 6mA [23]. Recent studies revealed that NMAD-1 is also controlling the DNA replication and repair in the meiosis phase in this organism [48]. On the other hand, unlike *E.coli* ALKB, the two AlkB homologs found in the *Schizosaccharomyces pombe* genome, Ofd2 and Abh1, have not activity repairing DNA lesions [49].

In the present study, we investigated the biological role of AlkB homologs in the physiology of *M. lusitanicus*. Bioinformatic analysis revealed three AlkB homologs in the *M. lusitanicus* genome, which conserved the AlkB domain. They were named *dmt1*, *dmt2*, and *dmt3*. *dmt2* and *dmt3* are closely related to human and mouse ALKBH1, while *dmt1* presented high similarity to N6-methyl adenine *demethylase* 1 (NMAD-1) of *C. elegans*. Deletion of these genes revealed that just *dmt1* is important for the appropriate dimorphic shift from yeast to mycelium and polar growth during the spore-macrophages interaction in *M. lusitanicus*. In addition, 6mA levels during the dimorphic transition were altered in *dmt1* deletion mutants, suggesting that 6mA regulates dimorphism in this fungus.

2. Materials and Methods

2.1. Fungal Strains and culture conditions

Mucor lusitanicus CBS277.49 [50] and the derived strain MU636 [51], a leucine auxotroph, were used as wild-type strain throughout this research. Strain MU402 [52], a uracil and leucine auxotroph, was used as recipient strain during genetic transformation to generate the *dmt* mutants.

All strains generated in this work are listed in Table S1. *M. lusitanicus* was grown in yeast extract peptone glucose (YPG; 3 g/l yeast extract, 10 g/L peptone, 20 g/L glucose, 15 g/L agar) medium agar plates or liquid, pH 4.5, to evaluate the sporulation, radial growth, and yeast to hyphae transition. The experiments to examine the effect of sodium dodecyl sulfate (SDS), DNA damaging agents, ultraviolet light, and prooxidants in *M. lusitanicus* were performed on Yeast Nitrogen Base (YNB; 1.5 g/L ammonium sulfate, 1.5 g/L glutamic acid, 0.5 g/L yeast nitrogen base without amino acids and ammonium sulfate, 10 g/L glucose, 15 g/L agar) medium, pH 3, supplemented with 1 ml thiamine (1 mg/ml) and niacin (1 mg/ml). Culture media were supplemented with uridine (200 mg/l) or leucine (20 mg/l) when necessary for auxotrophy complementation.

2.2. Disruption of dmt genes and generation of complemented strains

For single deletion of *M. lusitanicus dmt* genes, we constructed recombinant fragments by overlapping PCR. Constructs containing 2-kb sequence of the *pyrG* selectable marker flanked by 1-kb sequence up- and downstream of each *dmt* gene. Up- and downstream fragments of each *dmt* gene and *pyrG* gene were PCR amplified and subjected to overlap PCR using specific primers (Table S2) to obtain the deletion fragment. These constructs were used to genetically transform strain MU402 (*pyrG*-, *leuA*-) by electroporation to delete the target locus by homologous recombination [53]. Homokaryotic transformants (MU1316, MU1317, MU1318, MU1319, MU1320, and MU1321) were selected after several vegetive cycles on minimal medium with casamino acids (MMC), pH 3.2, supplemented with niacin (1 mg/ml) and thiamine (1 mg/ml) [54]. Gene deletion and homocaryosis were confirmed by Southern blot hybridization using specific probes.

To generate double knockout mutants, deletion fragments were generated as detailed previously. The *leuA* gene (3.2 kb in length) was surrounded by 1-kb up- and downstream sequences of the *dmt2* and *dmt3* genes that allowed the gene replacement by double

Preprints (www.preprints.org) | NOT PEER-REVIEWED | Posted: 23 July 2021 doi:10.20944/preprints202107.0525.v1

homologous recombination. These constructs were used for the genetic transformation of the recipient strain MU1317 for the generation of *dmt1Δ/dmt2Δ* mutant (MU1325 and MU1326) and *dmt1Δ/dmt3Δ* mutant (MU1322 and MU1323). The construct employed for *dmt3* deletion was also used for the transformation of mutant MU1318 to obtain the *dmt2Δ/dmt3Δ* double mutant (MU1328 and MU1330). Up- and downstream regions of *dmt* and *leuA* genes that constituted each of the constructs for gene deletion were amplified with specific primers (Table S2). Transformants were selected after several cycles of vegetative growth on YNB medium, pH 3, supplemented with niacin (1 mg/ml) and thiamine (1 mg/ml) [55].

To complement the MU1317 by reintroducing the *dmt1* wild-type allele, a construct was designed as follows: the *dmt1* open reading frame (ORF) including 1-kb 5′- and 3′-flanking regions were amplified from genomic DNA of *M. lusitanicus* CBS277.49 employing specific primers bearing XhoI and SacII restriction sites (Table S2). The *dmt1* fragment was cloned in the corresponding sites into the pMAT1476 plasmid [56], which contains the *leuA* selectable marker flanked by 5′- and 3′- ends of the *carRP* gene. The pMAT2250 plasmid constructed was digested with the *Sac*I and *Pvu*I restriction enzymes to release the whole construct that including the *leuA* cassette, *dmt1* allele, and *carRP* flanking sequences. The pMAT1476 plasmid was also digested with the *Sma*I enzyme to release the cassette containing only the *leuA* gene surrounded by *carRP* flanking sequences. The constructs were used to transform the MU1317 protoplast for its integration at the *carRP* locus. The transformants with correct integration developed colonies with white patches because of the deletion of the *carRP* gene. After several vegetative cycles on YNB medium [55], pH 3, supplemented with niacin (1 mg/ml) and thiamine (1 mg/ml), completely white colonies were obtained (MU1331 and MU1334), as a result of the homocaryosis confirmed by PCR (Table S1). The generation of protoplasts and the genetic transformation by electroporation were performed according to the previously described protocol [54].

2.3. *Southern blot*

To Southern blot hybridization, specific probes amplified from gDNA that discriminate between the wild type and mutant alleles were obtained by PCR amplification using the following specific primers: Udmt1F/Ddmt1-pyrGR, Udmt2F/Udmt2-pyrGR, and Udmt3F/Ddmt3-pyrGR for the genes *dmt1*, *dmt2,* and *dmt3*, respectively (Table S2). DNA probes were labeled using α-^{32}P dCTP employing Read-To-Go Labelling Beads (GE Healthcare Life Science). 1 µg of gDNA digested with restriction enzymes appropriated and separated by electrophoresis were transferred to an Amersham Hybond XL membrane (GE Healthcare Life Sciences) to the hybridization.

2.4. *Experiments of yeast to hyphae transition*

To induction of the yeast to hyphae transition, 1x10^6/ml fresh spores of different strains of *M. lusitanicus* were inoculated in 50 ml conical tubes filled with liquid YPG media pH 4.5 freshly autoclaved (warm) and sealed with parafilm. The cultures were incubated at 26°C without shaking for 24 h to yeast induction. 15 ml of the previous culture was poured into a 50 ml flask and placed in a shaker at 250 rpm and 26°C for 2.5 h for hyphal induction. The yeast and hyphae formed were observed by optical microscopy and photographed at 20 or 40X magnification. The percentage of cells with hyphae formation was calculated from 200 total cells. The polarity index was measured of 50 yeast with hyphae emergency using ImageJ software from micrographs taken 2.5 h after hyphal induction. The polarity index corresponded to the ratio between cell length and width. The statistical significance of each experiment was calculated using Tukey test ANOVA ($P < 0.001$) and unpaired t-test ($P < 0.05$).

2.5. *In vitro host-pathogen interaction assays*

To evaluate the survival of the *dmt* mutants *in vitro* host-pathogen interactions, fungal spores were co-inoculated with mouse macrophages J774A.1 in a ratio of 1:5

Preprints (www.preprints.org) | NOT PEER-REVIEWED | Posted: 23 July 2021 doi:10.20944/preprints202107.0525.v1

(spore:macrophage) in Leibovitz L-15 Medium at 37°C (Biowest) containing 10% fetal bovine serum (FBS) and 1% penicillin/streptomycin (Gibco). After 30 min, the cells were washed three times with 1X phosphate-buffered saline (PBS) to remove non-phagocytosed spores and placed at 37°C for 5.5 h. Macrophages were treated with 0.1% NP-40 cell lysis buffer to release the phagocytosed spores. 10 µl of each sample was seeded on MMC agar plates, pH 3.2, and incubated at 26°C for 48 h. The growth and development of healthy colonies were examined by visual inspection. Spores without macrophages cultured in L15 medium under the same conditions were employed as control. The micrographs of spore germination into macrophages taken 5.5 h of *in vitro* interaction were used to determine the polarity index from 50 spores as previously described.

2.6. *RNA extraction and cDNA synthesis*

The RNA extraction was carried out from samples collected several times (0 min, 30 min, 1 h, and 2 h) during the induction of yeast to hyphae transition by TRIzol method according to the supplier recommendation (Invitrogen). RNA concentration and quality were determined by spectrophotometric using Qubit fluorimeter (Invitrogen) and agarose gel electrophoresis, considering the 28S/18S rRNA ratio, respectively. 1 µg of total RNA was treated with TURBO DNase (Thermo Fisher) and was used for cDNA synthesis employing iScript cDNA Synthesis Kit (Bio-Rad) following the supplier recommendations. The cDNA synthesized was used as templated for real-time PCR assays.

2.7. *RT-qPCR analysis*

The transcriptional profile of the *pkaR4* gene was analyzed by qPCR at different times of induction of yeast to hyphae transition (0 min, 30 min, 1 h, and 2 h) with specific primers (Table 2). The gene amplification was carried out by triplicate using a reaction mixture containing 1X Power Sybr Green Master Mix 2X (Applied biosystem), 150 nM of *pkaR4*-specific primers, 100 ng cDNA templated. The real-time PCR was carried out using QuantStudio™ 5 real-time PCR system (Applied biosystem) according to the established experiment template in the equipment. Melting curve and non-template controls also measured to discern non-specific amplifications. The relative expression of *pkaR4* was normalized with the amplification levels of elongation factor 1 alpha gene (*ef-1*) [57] and calculated using the $2^{-\Delta\Delta CT}$ method [58].

2.8. *Analysis of 6mA in DNA by HPLC-MS*

Genomic DNA extracted from yeast and mycelia samples collected before (0 h) and after (2 h) dimorphism induction was digested to single nucleosides following previously established procedures [26,59]. 2 µg of gDNA diluted to a total volume of 26 µl with nuclease-free water were heated at 100ºC for 3 min and chilled on ice for 2 min. Treated DNA samples were digested with 1.5 U of DNAse I overnight at 42°C (ThermoFisher) and 0.001 U Phosphodiesterase I from *Crotalus adamanteus* venom to 37°C for 2 h (Merck) in 100 mM NH_4HCO_3 buffer, pH 7.8. Finally, digested gDNA was treated with 1 U of alkaline phosphatase at 37ºC for 2 h and diluted two-fold with nuclease-free water. Single nucleotides were analyzed using an HPLC-MS system consisting of an Agilent 1290 Infinity II Series HPLC (Agilent Technologies, Santa Clara, CA, USA) equipped with an Automated Multisampler module and a High-Speed BinaryPump, and connected to an Agilent 6550 Q-TOF Mass Spectrometer (Agilent Technologies, Santa Clara, CA, USA) using an Agilent Jet Stream Dual electrospray (AJS-Dual ESI) in the positive mode. Experimental parameters for HPLC and Q-TOF were set in MassHunter Workstation Data Acquisition software (Agilent Technologies, Rev. B.08.00). The nucleosides were quantified using the nucleoside to base ion mass transition of 252.1091 > 136.0638 m/z for dA ($C_{10}H_{13}N_5O_3$) and 266.1248 > 150.0812 m/z for 6mA ($C_{11}H_{15}N_5O_3$). The 6mA/dA ratio was calculated based on the concentration of each nucleoside.

2.9. *Sensitivity tests*

Preprints (www.preprints.org) | NOT PEER-REVIEWED | Posted: 23 July 2021 doi:10.20944/preprints202107.0525.v1

Different concentrations of fresh spore of analyzed strains (10^4, 10^3, 10^2, and 10 spores) were spotted on YNB agar plates, pH 3, amended with 0.005% SDS, 0.2% EMS, and 2 mg/ml HU. For Hydrogen peroxide (H_2O_2) and UV-associated assays, 200 spores were spread on YNB plates, pH 3, supplemented with 5 mM H_2O_2, or exposed to 10 mJ/cm^2 UV, respectively. All the plates were incubated at 26°C by 48 h to evaluate the *M. lusitanicus* ability to develop colonies in all conditions tested and estimate the survival percentage from total cells inoculated.

2. Results

3.1. Genes of M. lusitanicus encoding putative 6mA demethylases

We searched homologs of eukaryotic enzymes with demonstrated ability to remove methyl groups in the *M. lusitanicus* genome (CBS277.49 v2.0; https://mycocosm.jgi.doe.gov/Mucci2/Mucci2.home.html). A blast tool using *C. elegans* NMAD-1 [23] retrieved just one putative *M. lusitanicus* protein (FungiDB; QYA_85076), while a blast search with mouse ALKBH1 [43] identified two similar putative proteins in the fungus (FungiDB; QYA_106998 and QYA_115786). The deduced amino acid sequence of the three identified proteins contained the conserved domain 2-Oxoglutarate and Fe (II) dependent dioxygenase (2OG-FeII_Oxy_2), similar to the domain identified in known AlkB enzymes. The presence of this domain and their similarity with characterized 6mA demethylases suggested that they could be involved in removing methyl groups in 6mA [31,60], regulating in this way cellular processes of the fungus. The genes encoding these hypothetical proteins were named *dmt1* (FungiDB; QYA_85076), *dmt2* (FungiDB; QYA_106998), and *dmt3* (QYA_115786).

3.2. Generation of single and double dmt knockout mutants in M. lusitanicus

To analyse the function of the three *dmt* genes in *M. lusitanicus*, single and double mutants of each *demethylase* were generated by double homologous recombination. For single deletion mutants, disrupting fragments containing *pyrG* selectable marker were used for genetic transformation and replacement of each *dmt* gene in the strain MU402 (*pyr*G$^-$, *leu*A$^-$) (Figure S1). After several cycles of vegetative growth on selective media to isolate homokaryosis, two independent transformants of each knockout experiment were selected and analyzed by Southern blot hybridization. All transformants selected were homokaryons for the mutant allele because they only showed the hybridization fragment corresponding to the mutant allele (Figure S1). These single knockout mutants were named as follow: MU1316 and MU1317 had a deletion of *dmt1* gene, MU1318 and MU1319 had a deletion of *dmt2* gene, and MU1320 and MU1321 had a deletion of *dmt3 gene.*

Also, double knockout mutants in the *dmt* genes were generated from single deletion mutants (*pyr*G+, *leuA*-) by using recombinant fragments containing the selection marker *leuA*, which complement their leucine auxotrophy (Figure S2). Strain MU1317 (*dmt1Δ::pyr*G+, *leu*A-) was used as the recipient for the replacement of *dmt2* and *dmt3*. Two independent homokaryotic transformants were selected that carried deletion of *dmt1* and *dmt2* (MU1325 and MU1326) (Figure S2A) and another two having a deletion of *dmt1* and *dmt3* (MU1322 and MU1324) (Figure S2B). To generate the *dmt2Δ/dmt3Δ* knockout mutant, strain MU1319 (*dmt2Δ::pyr*G+, *leu*A-) was used for genetic transformation with recombinant fragment targeting the *dmt3* gene (Figure S2C). Two independent homokaryons (MU1328 and MU1330) were selected. Correctness of the deletions and homokaryosis were confirmed by PCR (Figure S2A-C). Both independent single and double deletion mutants were used to analyze the biological role of *M. lusitanicus dmt* genes in different conditions. However, in most experiments, just one member of each mutant pair was analyzed when no differences with the wild-type strains were found.

3.3. The dmt1 gene regulates the hyphae formation during the yeast to mycelium transition

Preprints (www.preprints.org) | NOT PEER-REVIEWED | Posted: 23 July 2021 doi:10.20944/preprints202107.0525.v1

To investigate if any of the three *dmt* genes play a role in the biology of *M. lusitanicus*, single and double deletion mutants were characterized phenotypically under different growth conditions. Single deletion mutants MU1317 (*dmt1*Δ), MU1318 (*dmt2*Δ), and MU1320 (*dmt3*Δ) showed colonial morphology, mycelial growth, and spore production similar to the wild-type strain MU636 (Figure S3A and S4A,B). Consistently, double deletion mutants MU1324 (*dmt1Δ/dmt3Δ*), MU1326 (*dmt1Δ/dmt2Δ*), and MU1330 (*dmt2Δ/dmt3Δ*) exhibited also parameters similar to the wild-type strain CBS277.49 (Figure S3B and S4C,D). Bacterial and mammals AlkB restoring DNA lesions induced alkylating agents, which double-strand breaks and replication inhibition of DNA [35,61]. Thus, strains were exposed to ethyl methane sulphonate (EMS) and Hydroxyurea (HU), which double-strand breaks and replication inhibition of DNA, respectively. *dmt* knockout strains show no changes in the sensitivity to EMS (0.2%) or HU (2 mg/ml) compared to the WT strain (Figure S5A,B). Similar behavior was observed in strains exposed to ultraviolet light (UV), while higher doses inhibited the growth of wild-type and mutant strains (Figure S6B). These data demonstrate that the pathway of DNA repair remained unaltered by the deletion of any *dmt* gene.

The presence of sodium dodecyl sulfate (SDS) (0.005%) in the culture medium to evaluate the integrity of the cell wall affected the growth of both single and double mutant similarly to WT strain (Figure S6A), which indicates that the integrity of the cell wall is not compromised with deletion of any of the three *dmt* genes. Later, the ability of *M. lusitanicus* to respond to stress conditions generated by hydrogen peroxide (H_2O_2) was tested; both the single and double knockout mutants presented a response equivalent to the wild-type strain to 5 mM H_2O_2 (Figure S6C). Taken together these data, suggest that the three *dmt* genes evaluated are not directly associated with the mechanism regulating the mycelial growth, spores production, DNA repair, cell wall integrity, and response to oxidative stress. Alternatively, redundancy among the three *dmt* genes could explain the wild-type phenotype of single and double deletion mutants.

M. lusitanicus has the ability to grow as yeast or hyphal depending on the environmental conditions and it is closely related to its virulence [13]. To evaluate the possible function of three *dmt* genes in dimorphism. The spores of the single and double *dmt* mutans were inoculated in YPG liquid culture medium, pH 4.5, in anaerobic conditions to induce yeast growth, and after 24 hours they were aerated by shaking at 250 rpm to stimulate the yeast to hyphae transition. Similarly to the wild-type strain, deletion mutants in the *dmt* genes showed markedly multi-budded yeast in anaerobic conditions, but when the transition from yeast to hyphae was induced, the two independent *dmt1* mutants MU1316 and MU1317 showed a delay in the emergence of the germination tube (Figure 1A,B). This phenotype was confirmed in the double mutants MU1326 (*dmt1Δ/dmt2Δ*) and MU1324 (*dmt1Δ/dmt3Δ*) harboring deletion of *dmt1*, but not in double deletion mutants for *dmt2* and *dmt3* (MU1330) (Figure 2A,B). We determined the polarity index, the ratio between cell length and width, to quantify polar growth to validate this phenotype. Interestingly, strains lacking *dmt1* presented an impaired polar growth than that of the wild-type strain (Figure 1C), suggesting that *dmt1* is important for the hyphal development of *M. lusitanicus* during the morphologic shift from yeast to hyphae.

Preprints (www.preprints.org) | NOT PEER-REVIEWED | Posted: 23 July 2021 doi:10.20944/preprints202107.0525.v1

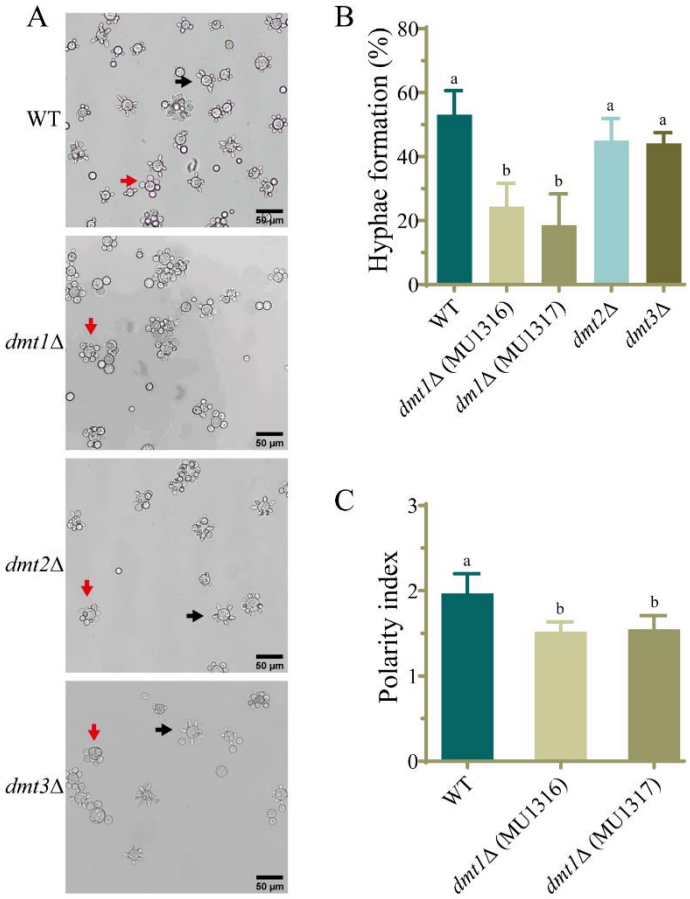

Figure 1. The mutants in the *dmt1* gene of *M. lusitanicus* are affected in the hyphae emergence during yeast to mycelium transition. A) Cells of wild-type strain MU636 (WT), *dmt1*Δ (MU1316 and MU1317), *dmt2*Δ (MU1318), and *dmt3*Δ (MU1320) 2.5 h after induction hyphal development by transferring to aerobics conditions. The arrows indicate the multi-budded yeasts (red) and cells with hyphae (black). B) The data represent the percentage of hyphae formation 2.5 h after transition induction calculated from 200 total cells. C) Polarity index quantified from 50 yeasts with hyphae emergency after 2.5 h induction. The charts display means ± SD. Different letters indicate statistically significant differences calculated using one-way ANOVA ($P < 0.001$). Three independent experiments were conducted for each strain.

Preprints (www.preprints.org) | NOT PEER-REVIEWED | Posted: 23 July 2021 doi:10.20944/preprints202107.0525.v1

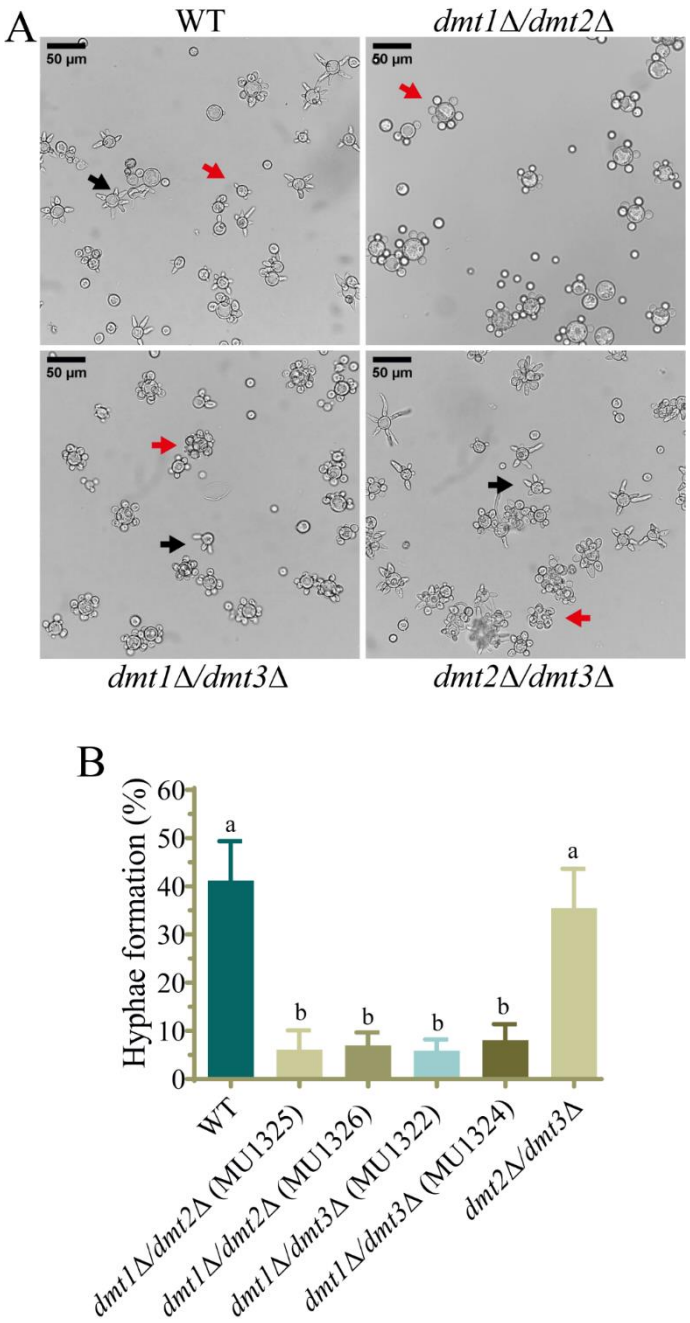

Figure 2. The double mutants having *dmt1* deletion were affected in the hyphae emergence during yeast to mycelium transition. A) Cells of wild-type strain CBS277.49 (WT), *dmt1*Δ/*dmt2*Δ (MU1325 and MU1326), *dmt1*Δ/*dmt3*Δ (MU1322 and MU1324), and *dmt2*Δ/*dmt3*Δ (MU1330) 2.5 h of growth after induction of hyphae formation by transferring to aerobics conditions. The arrows indicate the multi-budded yeasts (red) and cells with hyphae (black). B) Percentage of yeasts with developed hyphae in WT strain (CBS277.49) and the indicated double knockout mutants calculated from 200 total cells. The charts display means ± SD. Different letters indicate statistically significant differences calculated using one-way ANOVA ($P < 0.001$). Three independent experiments were conducted for each strain.

To test this hypothesis, the strain MU1317 (*dmt1Δ::pyrG*$^{+}$, *leuA*$^{-}$) was complemented with the wild-type *dmt1* gene. Construct containing the selective marker *leuA* and wild-type *dmt1* gene flanked by the 5'and 3' ends of the *carRP* gene was used for genetic transformation of MU1317 targeting the *carRP* gene, which codes for an enzyme required for carotenoid biosynthesis [62] (Figure S2D). As a control, a similar construct without *dmt1* gene was also used to transform MU1317 (Figure S2E). Transformants with albino

Preprints (www.preprints.org) | NOT PEER-REVIEWED | Posted: 23 July 2021 doi:10.20944/preprints202107.0525.v1

patches, due to the disruption of the *carRP* gene, were grown on a selective medium to obtain homokaryotic strains that were analyzed by PCR to confirm the gene replacement (Figure S2D,E). One homokaryotic strain harboring the wild-type *dmt1* allele (MU1331) and one control strain (MU1334) containing the only selective marker *leuA* were selected for further analysis (Figure S2D,E and S3C). The strain harboring the wild-type *dmt1* allele recovered the ability to develop hyphae after transition induction. In contrast, control strain MU1334 exhibited a similar phenotype to the *dmt1* mutant (Figure 3A,B), supporting *dmt1* plays a key role in the dimorphic transition from yeast to mycelium of *M. lusitanicus*.

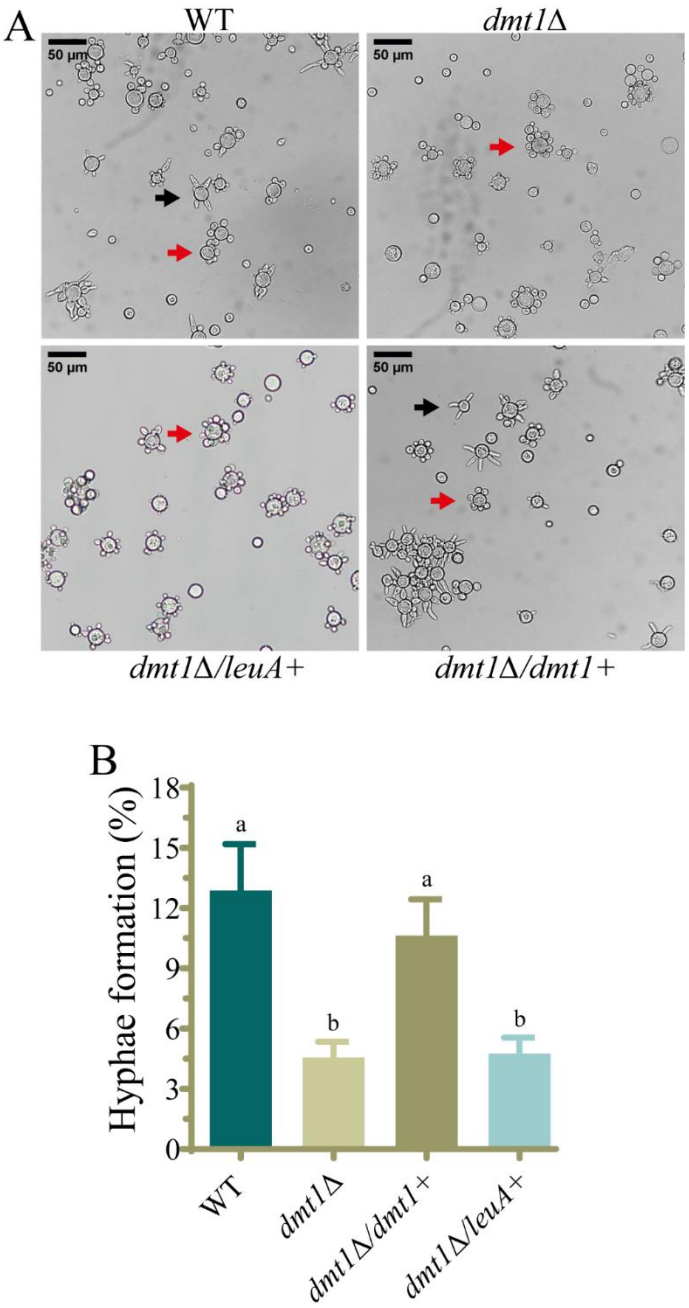

Figure 3. Complementation of *dmt1* mutant with the wild-type allele of *dmt1* gene recovered the ability to develop hyphae. A) Cells of the wild-type strain MU636 (WT), *dmt1*Δ (MU1317), *dmt1*Δ complemented with *dmt1* wild-type allele (MU1331), and *dmt1*Δ complemented with empty vector (MU1334) 2.5 h after induction of mycelial growth by transferring to aerobics conditions. The arrows indicate the multipolar budding yeasts (red) and cells with germinated hyphae (black). B) Percentage of yeasts with developed hyphae in WT strain and the indicated strains calculated from 200 total cells. The charts display means ± SD. Different letters indicate statistically significant differences

Preprints (www.preprints.org) | NOT PEER-REVIEWED | Posted: 23 July 2021 doi:10.20944/preprints202107.0525.v1

calculated using one-way ANOVA ($P < 0.001$). Three independent experiments were conducted for each strain.

3.4. The dmt1 regulates the pkaR4 transcription during the transition from yeast to hyphae

To further support the function of *dmt1* in dimorphism, we analyzed the mRNA accumulation of *pkaR4*, a gene encoding one regulatory subunit of cAMP-dependent protein kinase A (PKA) required for germ tube emergence in aerobic conditions [15]. To that end, yeast cells of *dmt1*Δ and the complemented strain were transferred from anaerobic to aerobic conditions to induce hyphal growth and samples were taken at different times (0 min, 30 min, 1 h, and 2 h). In the early times after induction of the dimorphic transition (30 min and 1 h), *pkaR4* transcript levels remained unaltered in comparison to the yeast form (0 min) in all tested strains, but after 2 h, *pkaR4* mRNA levels increased 11.5 folds in the wild-type strain (Figure 4A). Interestingly, at this time, the *pkaR4* transcript levels in the *dmt1*Δ strain were significantly lower (6.5-fold increase) (Figure 4A), suggesting that *dmt1* regulates *pkaR4* expression. This result was further confirmed with the quantification of *pkaR4* expression in the strain that expressed ectopically *dmt1* because a partial recovered of the *pkaR4* expression (8.3-fold increase) was observed, whereas its control (MU1334) in which only the *leuA* marker display similar induction as the *dmt1* mutant (Figure 4A). In consequence, these results suggest that *dmt1* controls germ tube emergence in the dimorphic transition of *M. lusitanicus* by regulating the expression of *pkaR4*.

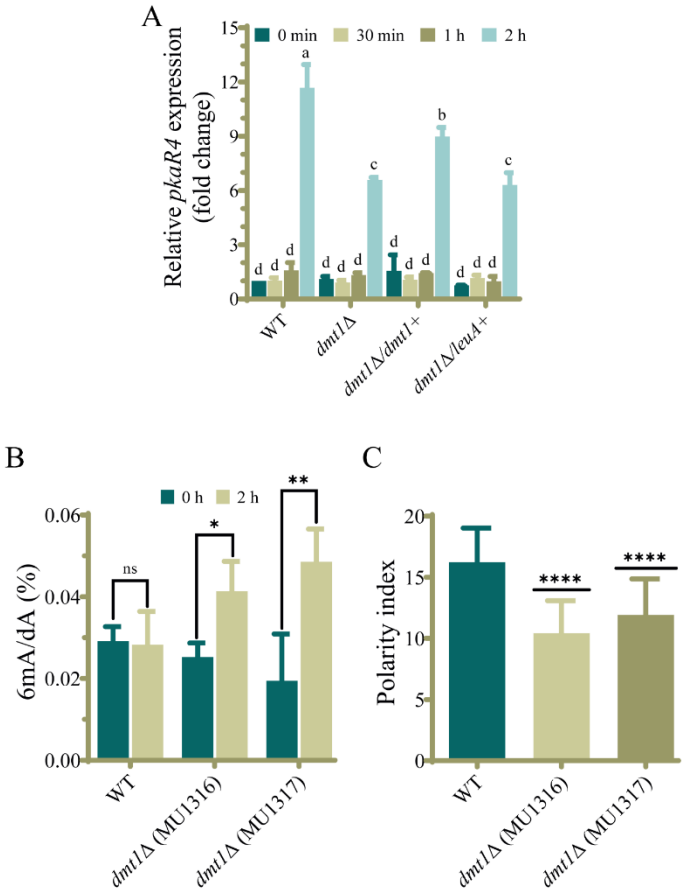

Figure 4. The gene *dmt1* is required for appropriate expression of the *pkaR4* gene during yeast to hyphae transition. A) mRNA levels of *pkaR4* were determined by RT-PCR from total RNA isolated from MU636 (WT), *dmt1*Δ (MU1317), *dmt1*Δ complemented with *dmt1* wild-type allele (MU1331), and *dmt1*Δ complemented with empty vector (MU1334) at different times (0 min, 30 min, 1 h, and 2 h) after induction of transition from yeast to mycelium. The amplification levels of *ef-1* were used to normalize the relative expression of *pkaR4* using the $2^{-\Delta\Delta CT}$ method. B) 6mA levels, determined by HPLC-MS analysis, in genomic DNA isolated from yeast cells before (0 h) and 2 h after transferring them to aerobic conditions of the wild type strain MU636 (WT) and *dmt1* mutants (MU1316 and

 doi:10.20944/preprints202107.0525.v1

MU1317). C) Polarity index of the wild-type strain MU636 (WT) and *dmt1* mutants MU1316 and MU1317 measured 5.5 h after phagocytosis by mouse macrophages line J774A.1. The polarity index was calculated from 50 phagocytosed spores. The charts display means ± SD. Different letters and asterisks indicate statistically significant differences calculated using one-way ANOVA ($P < 0.001$) and unpaired t-test ($P < 0.05$; ns, not significant).

3.5. Deletion of dmt1 alters 6mA levels during yeast to hyphae transition

The protein encoded by *dmt1* is highly similar to AlkB proteins from eukaryotes, particularly to the *C. elegans* NMAD-1, which demethylates 6mA in DNA. Therefore, we hypothesized that Dmt1 could also remove this epigenetic mark in DNA. Thus, we measured 6mA levels in yeasts and 2 h after the transition to aerobic conditions by HPLC-MS in *dmt1* mutants and the wild-type strain. The genomic 6mA levels were similar in both conditions in the wild-type strain (Figure 4B), indicating that 6mA is maintained during the dimorphic transition. Interestingly and in contrast to the wild-type strain, both *dmt1* mutants showed an increase in the 6mA levels only after the transition (Figure 4B), suggesting that *dmt1* gene is required to sustain the 6mA levels during the transition from yeast to hyphae.

3.6. dmt1 regulates germination in the interaction of spores with macrophages in vitro

Because the *dmt1* mutants showed a delay in the hyphae formation during yeast to hyphal transition, we hypothesized that this phenomenon could impact the ability of *M. lusitanicus* spores to survive during the macrophage interaction and escape phagocytosis. To support this hypothesis, fresh spores of *dmt1* mutants MU1316 and MU1317 were co-inoculated with mouse macrophages in a cell culture medium. The *dmt1* deletion did not affect the ability of *M. lusitanicus* to survive the cytotoxic environment of the macrophage's phagocytosis because spores collected after 5 h of interaction developed healthy colonies similar to the wild-type strain (data not shown). However, the germination capacity inside the phagosome was slightly affected during the co-culture with macrophages as the polarity index *dmt1* mutants was lower than that of the wild-type strain (Figure 4C). This delay in germination suggests that *dmt1* plays a role in this process and can be important in the course of the infection.

4. Discussion

A high density of 6mA has been associated with active transcription in early-diverging fungi [25], suggesting enzymes that modify its levels in the genome could regulate cell processes by regulating transcription in this group of fungal lineages, which includes Mucorales. In the present study, we analyzed the function in *M. lusitanicus* of three genes, *dmt1*, *dmt2*, and *dmt3*, encoding putative 6mA demethylases because of their similarity with known eukaryotic 6mA demethylases. Gene products of *dmt2* and *dmt3* were closely related to humans and mouse ALKBH1, while *dmt1* was similar to *C. elegans* NMAD-1. The NMAD-1 deletion causes a high accumulation of 6mA in *C. elegans*, indicating that this enzyme is the main demethylase of this epigenetic mark [23,63]. An event similar has been reported to mammalian ALKBH1 [43]. The three Dmt protein sequences include an AlkB domain found in ALKB enzymes responsible for removing the methyl group of DNA [23,63], playing important roles in several biological processes in both prokaryotes and eukaryotes [31]. These findings suggested that the products of some *dmt* genes could act in a similar way to NMAD-1 and ALKBH1 and regulate cellular processes in *M. lusitanicus*.

Phenotypes previously related to AlkB proteins such as sporulation, growth, and DNA repair [35,61,64] were unaltered in mutants with a deletion in one or two *dmt* genes. This result could be explained considering that these genes are unlinked to the studied processes or their functions overlap. Interestingly, the deletion of *dmt1* either alone or in combination with *dmt2* or *dmt3* leads to a delay in germination tube emission during the dimorphic transition from yeast to mycelium. In contrast, single deletion of *dmt2* and *dmt3* or deletion of both genes produced a wild-type phenotype (Figure 1 and 2), suggesting that the defect in dimorphism was due exclusively to the absence of *dmt1*. This hypothesis

Preprints (www.preprints.org) | NOT PEER-REVIEWED | Posted: 23 July 2021 doi:10.20944/preprints202107.0525.v1

was further supported by reversing the defect in strains that expressed *dmt1* wild-type allele ectopically (Figure 3). These findings evidence a central role of this *dmt1* in the control of morphogenesis in *M. lusitanicus*, probably through regulating the expression of genes involved in the transition from yeasts to mycelium. This regulation could be mediated by modifying the 6mA pattern of genes involved in the transition. Therefore, we measured the total 6mA levels in the wild-type strain and *dmt1* mutants during the transition from yeast to mycelium. In contrast to the wild-type strain, which maintained similar 6mA levels during the transition, the *dmt1* mutants showed an increase after mycelial growth was induced (Figure 4B), suggesting that there was an over-methylation in the absence of *dmt1* that could affect the expression of some genes involved in the dimorphism. These results hint at *dmt1* encoding a 6mA demethylase that regulates the expression of some critical genes during the transition from yeast to mycelium by lowering their 6mA levels during the transition.

In recent years, mucormycosis has become one of the main invasive fungal infections due to its rapid growth and its ability to shift morphologically during infection [8]. The substantial contribution of the morphological shift from yeast to hyphae of *M. lusitanicus* to its virulence and pathogenesis [65] makes dimorphism a promising target for treating mucormycosis and the design of new antifungal drugs [13,14]. A few proteins regulating dimorphism have been characterized, the most remarkable being Calcineurin and PKA. Strains lacking the calcineurin regulatory B subunit (CnbR) remain in the yeast form and show reduced virulence [13,14], while strains lacking the catalytic A subunit (CnaA) remain in the filamentous phase and show high virulence [13]. In addition, this fungus has four genes encoding regulatory subunits of PKA with different roles in physiology [15]. One of these genes, *pkaR4*, is transcribed exclusively during morphogenesis from yeast to mycelium and plays a critical role in mycelial growth as its deletion prevents mycelial growth, whereas overexpression promotes filamentous growth [15,16]. As previously described, we found low expression levels of *pkaR4* in yeasts and a sharp increase when filamentous growth started (Figure 4A). Although *dmt1* mutants also showed an increase of *pkaR4* transcripts during the transition, the induction was lower than in the wild-type and complemented strains, suggesting that *dmt1* regulates directly or indirectly *pkaR4* expression. The reduced *pkaR4* expression in *dmt1* mutants could be responsible for the delay in germ tube development during the transition from yeast to mycelium.

In addition to the function of *dmt1* in dimorphism, it is also involved in spore germination during interaction with macrophages because spores of the *dmt1* mutants showed a delay in germination, evidenced by a low polarity index (Figure 4C). *M. lusitanicus* strains exhibiting a low polarity index in the interaction with macrophages also present reduced virulence [66]. Accordingly, the delayed polar growth due to the disruption of the *dmt1* gene could affect the virulence of *M. lusitanicus*. The role of epigenetic modifications in the control of cellular processes, including virulence, has not been studied in early-diverging fungi. Consequently, this work represents the first study describing the function of a gene that modifies the DNA. Further analysis to reveal the gene network mediated by *dmt* regulation could be necessary to understand all the implications of *dmt1* in gene expression regulation.

Supplementary Materials: The following are available online at www.mdpi.com/xxx/s1, Figure S1: Gene replacement by homologous recombination of the *dmt* genes in *M. lusitanicus*, Table S1: Mutants generated in this study, Figure S2: Generation of *dmt* double mutants and complementation of strain MU1317 (*dmt1*Δ) with *dmt1* wild-type allele, Table S2: Primers used in this work, Figure S3: Phenotypic analysis of *dmt* mutants and complemented strains, Figure S4: Single and double deletion mutants in the *dmt* genes are not affected in the growth and sporulation. Figure S5: Phenotypic analysis of single deletion mutants in the *dmt1*, *dmt2*, and *dmt3* genes exposed to alkylating agents and compounds inhibiting DNA synthesis, Figure S6: Survival analysis of single deletion mutants in the *dmt1*, *dmt2*, and *dmt3* genes exposed to stress generating compounds and DNA damaging agents

Author Contributions. Conceptualization, V.G and F.E.N.; methodology, M.O.C., C.L., E.N. and F.E.N.; validation, V.G., F.E.N.; formal analysis, M.O.C., C.L., F.E.N. and V.G.; investigation, M.O.C., C.L., E.N. and F.E.N.; resources, V.G., F.E.N. and E.N.; data curation, M.O.C., C.L. and V.G.; writing—original draft preparation, M.O.C. and C.L..; writing—review and editing, V.G., F.E.N. and E.N.; supervision, V.G. and F.E.N.; project administration, V.G.; funding acquisition, V.G. All authors have read and agreed to the published version of the manuscript.

Funding: This research was funded by Fundación Séneca-Agencia de Ciencia y Tecnología de la Región de Murcia, Spain (20897/PI/18). M.O.C. was supported by posdoctoral fellowship from Consejo Nacional de Ciencia y Tecnología (CONACYT), México (No. 711112 and 740510). C.L. was supported by predoctoral fellowship from Ministerio de Ciencia, Innovación y Universidades (MCIU), Spain (FPU17/05814).

Institutional Review Board Statement Not applicable

Informed Consent Statement: Not applicable

Data Availability Statement: Not applicable

Acknowledgments: This work was supported by the Fundación Séneca-Agencia de Ciencia y Tecnología de la Región de Murcia, Spain (20897/PI/18). M.O.C. acknowledges CONACYT for the postdoctoral fellowship (711112 and 740510).

Conflicts of Interest: The authors declare no conflict of interest. The funders had no role in the design of the study; in the collection, analyses, or interpretation of data; in the writing of the manuscript, or in the decision to publish the results.

References

1. Gleissner, B.; Schilling, A.; Anagnostopolous, I.; Siehl, I.; Thiel, E. Improved Outcome of Zygomycosis in Patients with Hematological Diseases? *Leuk. Lymphoma* **2004**, *45*, 1351–1360, doi:10.1080/10428190310001653691.
2. Brown, G.D.; Denning, D.W.; Levitz, S.M. Tackling human fungal infections. *Science* **2012**, *336*, 647, doi:10.1126/science.1222236.
3. Binder, U.; Maurer, E.; Lass-Flörl, C. Mucormycosis – from the pathogens to the disease. *Clin. Microbiol. Infect.* **2014**, *20*, 60–66, doi:10.1111/1469-0691.12566.
4. Veisi, A.; Bagheri, A.; Eshaghi, M.; Rikhtehgar, M.H.; Rezaei Kanavi, M.; Farjad, R. Rhino-orbital mucormycosis during steroid therapy in COVID-19 patients: A case report. *Eur. J. Ophthalmol.* **2021**, 112067212110094, doi:10.1177/11206721211009450.
5. John, T.M.; Jacob, C.N.; Kontoyiannis, D.P. When Uncontrolled Diabetes Mellitus and Severe COVID-19 Converge: The Perfect Storm for Mucormycosis. *J. Fungi* **2021**, *7*, 298, doi:10.3390/jof7040298.
6. Kauffman, C.A. Zygomycosis: Reemergence of an old pathogen. *Clin. Infect. Dis.* **2004**, *39*, 588–590, doi:10.1086/422729.
7. Lebreton, A.; Corre, E.; Jany, J.-L.; Brillet-Guéguen, L.; Pèrez-Arques, C.; Garre, V.; Monsoor, M.; Debuchy, R.; Meur, C. Le; Coton, E.; et al. Comparative genomics applied to Mucor species with different lifestyles. *BMC Genomics 2020 211* **2020**, *21*, 1–21, doi:10.1186/S12864-019-6256-2.
8. Ibrahim, A.S.; Voelz, K. The mucormycete–host interface. *Curr. Opin. Microbiol.* **2017**, *40*, 40–45, doi:10.1016/J.MIB.2017.10.010.
9. Lax, C.; Pérez-arques, C.; Navarro-mendoza, M.I.; Cánovas-márquez, J.T.; Tahiri, G.; Pérez-ruiz, J.A.; Osorio-concepción, M.; Murcia-flores, L.; Navarro, E.; Garre, V.; et al. Genes, pathways, and mechanisms involved in the virulence of mucorales. *Genes (Basel).* **2020**, *11*, 317, doi:10.3390/genes11030317.
10. Orlowski, M. Mucor dimorphism. *Microbiol. Rev.* **1991**, *55*, 234–58.
11. Wolff, A.M.; Appel, K.F.; Petersen, J.B.; Poulsen, U.; Arnau, J. Identification and analysis of genes involved in the control of dimorphism in Mucor circinelloides (syn. racemosus) . *FEMS Yeast Res.* **2002**, *2*, 203–213, doi:10.1111/j.1567-1364.2002.tb00085.x.
12. Boyce, K.J.; Andrianopoulos, A. Fungal dimorphism: The switch from hyphae to yeast is a specialized morphogenetic adaptation allowing colonization of a host. *FEMS Microbiol. Rev.* 2015, *39*, 797–811.

13. Lee, S.C.; Li, A.; Calo, S.; Heitman, J. Calcineurin Plays Key Roles in the Dimorphic Transition and Virulence of the Human Pathogenic Zygomycete Mucor circinelloides. *PLoS Pathog.* **2013**, *9*, e1003625, doi:10.1371/journal.ppat.1003625.
14. Lee, S.C.; Li, A.; Calo, S.; Inoue, M.; Tonthat, N.K.; Bain, J.M.; Louw, J.; Shinohara, M.L.; Erwig, L.P.; Schumacher, M.A.; et al. Calcineurin orchestrates dimorphic transitions, antifungal drug responses and host-pathogen interactions of the pathogenic mucoralean fungus Mucor circinelloides. *Mol. Microbiol.* **2015**, *97*, 844–865, doi:10.1111/mmi.13071.
15. Ocampo, J.; Nuñez, L.F.; Silva, F.; Pereyra, E.; Moreno, S.; Garre, V.; Rossi, S. A subunit of protein kinase a regulates growth and differentiation in the fungus mucor circinelloides. *Eukaryot. Cell* **2009**, *8*, 933–944, doi:10.1128/EC.00026-09.
16. Ocampo, J.; McCormack, B.; Navarro, E.; Moreno, S.; Garre, V.; Rossi, S. Protein kinase A regulatory subunit isoforms regulate growth and differentiation in Mucor circinelloides: Essential role of pkaR4. *Eukaryot. Cell* **2012**, *11*, 989–1002, doi:10.1128/EC.00017-12.
17. Robbins, N.; Leach, M.D.; Cowen, L.E. Lysine Deacetylases Hda1 and Rpd3 Regulate Hsp90 Function thereby Governing Fungal Drug Resistance. *Cell Rep.* **2012**, *2*, 878–888, doi:10.1016/j.celrep.2012.08.035.
18. Hnisz, D.; Bardet, A.F.; Nobile, C.J.; Petryshyn, A.; Glaser, W.; Schöck, U.; Stark, A.; Kuchler, K. A Histone Deacetylase Adjusts Transcription Kinetics at Coding Sequences during Candida albicans Morphogenesis. *PLoS Genet.* **2012**, *8*, e1003118, doi:10.1371/journal.pgen.1003118.
19. Nobile, C.J.; Fox, E.P.; Hartooni, N.; Mitchell, K.F.; Hnisz, D.; Andes, D.R.; Kuchler, K.; Johnson, A.D. A histone deacetylase complex mediates biofilm dispersal and drug resistance in Candida albicans. *MBio* **2014**, *5*, doi:10.1128/mBio.01201-14.
20. Sedgwick, B.; Bates, P.A.; Paik, J.; Jacobs, S.C.; Lindahl, T. Repair of alkylated DNA: Recent advances. *DNA Repair (Amst).* **2007**, *6*, 429–442, doi:10.1016/j.dnarep.2006.10.005.
21. Iyer, L.M.; Abhiman, S.; Aravind, L. Natural history of eukaryotic DNA methylation systems. In *Progress in Molecular Biology and Translational Science*; Elsevier B.V., 2011; Vol. 101, pp. 25–104.
22. Bird, A. DNA methylation patterns and epigenetic memory. *Genes Dev.* 2002, *16*, 6–21.
23. Greer, E.L.; Blanco, M.A.; Gu, L.; Sendinc, E.; Liu, J.; Aristizábal-Corrales, D.; Hsu, C.-H.; Aravind, L.; He, C.; Shi, Y. DNA Methylation on N6-Adenine in C. elegans. *Cell* **2015**, *161*, 868–878, doi:10.1016/j.cell.2015.04.005.
24. Koziol, M.J.; Bradshaw, C.R.; Allen, G.E.; Costa, A.S.H.; Frezza, C.; Gurdon, J.B. Identification of methylated deoxyadenosines in vertebrates reveals diversity in DNA modifications. *Nat. Struct. Mol. Biol.* **2016**, *23*, 24–30, doi:10.1038/nsmb.3145.
25. Mondo, S.J.; Dannebaum, R.O.; Kuo, R.C.; Louie, K.B.; Bewick, A.J.; LaButti, K.; Haridas, S.; Kuo, A.; Salamov, A.; Ahrendt, S.R.; et al. Widespread adenine N6-methylation of active genes in fungi. *Nat. Genet.* **2017**, *49*, 964–968, doi:10.1038/ng.3859.
26. Fu, Y.; Luo, G.Z.; Chen, K.; Deng, X.; Yu, M.; Han, D.; Hao, Z.; Liu, J.; Lu, X.; Doré, L.C.; et al. N6-methyldeoxyadenosine marks active transcription start sites in Chlamydomonas. *Cell* **2015**, *161*, 879–892, doi:10.1016/j.cell.2015.04.010.
27. Beh, L.Y.; Debelouchina, G.T.; Clay, D.M.; Thompson, R.E.; Lindblad, K.A.; Hutton, E.R.; Bracht, J.R.; Sebra, R.P.; Muir, T.W.; Landweber, L.F. Identification of a DNA N6-adenine methyltransferase complex and its impact on chromatin organization. *Cell* **2019**, *177*, 1781-1796.e25, doi:10.1016/j.cell.2019.04.028.
28. Luo, G.Z.; Hao, Z.; Luo, L.; Shen, M.; Sparvoli, D.; Zheng, Y.; Zhang, Z.; Weng, X.; Chen, K.; Cui, Q.; et al. N 6-methyldeoxyadenosine directs nucleosome positioning in Tetrahymena DNA 06 Biological Sciences 0604 Genetics. *Genome Biol.* **2018**, *19*, 1–12, doi:10.1186/s13059-018-1573-3.
29. O'Brown, Z.K.; Greer, E.L. N6-methyladenine: A conserved and dynamic DNA mark. *Adv. Exp. Med. Biol.* **2016**, *945*, 213–246, doi:10.1007/978-3-319-43624-1_10.
30. Duncan, T.; Trewick, S.C.; Koivisto, P.; Bates, P.A.; Lindahl, T.; Sedgwick, B. Reversal of DNA alkylation damage by two human dioxygenases. *Proc. Natl. Acad. Sci. U. S. A.* **2002**, *99*, 16660–16665, doi:10.1073/pnas.262589799.
31. Fedeles, B.I.; Singh, V.; Delaney, J.C.; Li, D.; Essigmann, J.M. The AlkB family of Fe(II)/α-ketoglutarate-dependent dioxygenases: Repairing nucleic acid alkylation damage and beyond. *J. Biol. Chem.* 2015, *290*, 20734–20742.
32. Kamat, S.S.; Fan, H.; Sauder, J.M.; Burley, S.K.; Shoichet, B.K.; Sali, A.; Raushel, F.M. Enzymatic deamination of the epigenetic

base N-6-methyladenine. *J. Am. Chem. Soc.* **2011**, *133*, 2080–2083, doi:10.1021/ja110157u.

33. Chen, K.; Luo, G.Z.; He, C. High-Resolution Mapping of N6-Methyladenosine in Transcriptome and Genome Using a Photo-Crosslinking-Assisted Strategy. In *Methods in Enzymology*; Academic Press Inc., 2015; Vol. 560, pp. 161–185.
34. Van den Born, E.; Bekkelund, A.; Moen, M.N.; Omelchenko, M. V.; Klungland, A.; Falnes, P. Bioinformatics and functional analysis define four distinct groups of AlkB DNA-dioxygenases in bacteria. *Nucleic Acids Res.* **2009**, *37*, 7124–7136, doi:10.1093/nar/gkp774.
35. Aas, P.A.; Otterlei, M.; Falnes, P.; Vågbø, C.B.; Skorpen, F.; Akbari, M.; Sundheim, O.; Bjørås, M.; Slupphaug, G.; Seeberg, E.; et al. Human and bacterial oxidative demethylases repair alkylation damage in both RNA and DNA. *Nature* **2003**, *421*, 859–863, doi:10.1038/nature01363.
36. Korvald, H.; Mølstad Moe, A.M.; Cederkvist, F.H.; Thiede, B.; Laerdahl, J.K.; Bjørås, M.; Alseth, I. Schizosaccharomyces pombe Ofd2 Is a Nuclear 2-Oxoglutarate and Iron Dependent Dioxygenase Interacting with Histones. *PLoS One* **2011**, *6*, e25188, doi:10.1371/journal.pone.0025188.
37. Meza, T.J.; Moen, M.N.; Vågbo, C.B.; Krokan, H.E.; Klungland, A.; Grini, P.E.; Falnes, P.O. The DNA dioxygenase ALKBH2 protects Arabidopsis thaliana against methylation damage. *Nucleic Acids Res.* **2012**, *40*, 6620–6631, doi:10.1093/nar/gks327.
38. Tsujikawa, K.; Koike, K.; Kitae, K.; Shinkawa, A.; Arima, H.; Suzuki, T.; Tsuchiya, M.; Makino, Y.; Furukawa, T.; Konishi, N.; et al. Expression and sub-cellular localization of human ABH family molecules. *J. Cell. Mol. Med.* **2007**, *11*, 1105–1116, doi:10.1111/j.1582-4934.2007.00094.x.
39. Ougland, R.; Rognes, T.; Klungland, A.; Larsen, E. Non-homologous functions of the AlkB homologs. *J. Mol. Cell Biol.* 2015, *7*, 494–504.
40. Sundheim, O.; Vågbø, C.B.; Bjørås, M.; Sousa, M.M.L.; Talstad, V.; Aas, P.A.; Drabløs, F.; Krokan, H.E.; Tainer, J.A.; Slupphaug, G. Human ABH3 structure and key residues for oxidative demethylation to reverse DNA/RNA damage. *EMBO J.* **2006**, *25*, 3389–3397, doi:10.1038/sj.emboj.7601219.
41. Liu, Y.; Yuan, Q.; Xie, L. The AlkB Family of Fe (II)/Alpha-Ketoglutarate-Dependent Dioxygenases Modulates Embryogenesis through Epigenetic Regulation. *Curr. Stem Cell Res. Ther.* **2018**, *13*, doi:10.2174/1574888x12666171027105532.
42. Ma, C.-J.; Ding, J.-H.; Ye, T.-T.; Yuan, B.-F.; Feng, Y.-Q. AlkB homologue 1 demethylates N3-methylcytidine in mRNA of mammals. *ACS Chem. Biol.* **2019**, *14*, 1418–1425, doi:10.1021/acschembio.8b01001.
43. Wu, T.P.; Wang, T.; Seetin, M.G.; Lai, Y.; Zhu, S.; Lin, K.; Liu, Y.; Byrum, S.D.; Mackintosh, S.G.; Zhong, M.; et al. DNA methylation on N6-adenine in mammalian embryonic stem cells. *Nature* **2016**, *532*, 329–333, doi:10.1038/nature17640.
44. Nigam, R.; Babu, K.R.; Ghosh, T.; Kumari, B.; Akula, D.; Rath, S.N.; Das, P.; Anindya, R.; Khan, F.A. Indenone derivatives as inhibitor of human DNA dealkylation repair enzyme AlkBH3. *Bioorganic Med. Chem.* **2018**, *26*, 4100–4112, doi:10.1016/j.bmc.2018.06.040.
45. Pilžys, T.; Marcinkowski, M.; Kukwa, W.; Garbicz, D.; Dylewska, M.; Ferenc, K.; Mieczkowski, A.; Kukwa, A.; Migacz, E.; Wołosz, D.; et al. ALKBH overexpression in head and neck cancer: potential target for novel anticancer therapy. *Sci. Rep.* **2019**, *9*, 1–16, doi:10.1038/s41598-019-49550-x.
46. Nordstrand, L.M.; Svärd, J.; Larsen, E.; Nilsen, A.; Ougland, R.; Furu, K.; Lien, G.F.; Rognes, T.; Namekawa, S.H.; Lee, J.T.; et al. Mice Lacking Alkbh1 Display Sex-Ratio Distortion and Unilateral Eye Defects. *PLoS One* **2010**, *5*, e13827, doi:10.1371/journal.pone.0013827.
47. Kawarada, L.; Suzuki, T.; Ohira, T.; Hirata, S.; Miyauchi, K.; Suzuki, T. ALKBH1 is an RNA dioxygenase responsible for cytoplasmic and mitochondrial tRNA modifications. *Nucleic Acids Res.* **2017**, *45*, 7401–7415, doi:10.1093/nar/gkx354.
48. Yuan Wang, S.I.; Mao, H.I.; Shibuya, H.I.; Uzawa, S.I.; Klapholz, Z.O.; Wesenberg, S.; ShinID, N.; Saito, T.T.; Gao, J.; Meyer, B.J.; et al. The demethylase NMAD-1 regulates DNA replication and repair in the Caenorhabditis elegans germline. **2019**, doi:10.1371/journal.pgen.1008252.
49. Korvald, H.; Falnes, P.; Laerdahl, J.K.; Bjørås, M.; Alseth, I. The Schizosaccharomyces pombe AlkB homolog Abh1 exhibits

AP lyase activity but no demethylase activity. *DNA Repair (Amst).* **2012**, *11*, 453–462, doi:10.1016/j.dnarep.2012.01.014.

50. Schipper, M.A.A. On Mucor circinelloides, Mucor racemosus and Related Species. *Stud. Mycol.* **1976**, *12*, 1–40, doi:10.1016/s0007-1536(76)80201-x.
51. Navarro-Mendoza, M.I.; Pérez-Arques, C.; Panchal, S.; Nicolás, F.E.; Mondo, S.J.; Ganguly, P.; Pangilinan, J.; Grigoriev, I. V.; Heitman, J.; Sanyal, K.; et al. Early Diverging Fungus Mucor circinelloides Lacks Centromeric Histone CENP-A and Displays a Mosaic of Point and Regional Centromeres. *Curr. Biol.* **2019**, *29*, 3791-3802.e6, doi:10.1016/j.cub.2019.09.024.
52. Nicolás, F.E.; de Haro, J.P.; Torres-Martínez, S.; Ruiz-Vázquez, R.M. Mutants defective in a Mucor circinelloides dicer-like gene are not compromised in siRNA silencing but display developmental defects. *Fungal Genet. Biol.* **2007**, *44*, 504–516, doi:10.1016/j.fgb.2006.09.003.
53. Gutiérrez, A.; López-García, S.; Garre, V. High reliability transformation of the basal fungus Mucor circinelloides by electroporation. *J. Microbiol. Methods* **2011**, *84*, 442–446, doi:10.1016/j.mimet.2011.01.002.
54. Vellanki, S.; Navarro-Mendoza, M.I.; Garcia, A.; Murcia, L.; Perez-Arques, C.; Garre, V.; Nicolas, F.E.; Lee, S.C. *Mucor circinelloides* : Growth, Maintenance, and Genetic Manipulation. *Curr. Protoc. Microbiol.* **2018**, *49*, e53, doi:10.1002/cpmc.53.
55. Nicolás, F.E.; Navarro-Mendoza, M.I.; Pérez-Arques, C.; López-García, S.; Navarro, E.; Torres-Martínez, S.; Garre, V. Molecular tools for carotenogenesis analysis in the mucoral Mucor circinelloides. In *Methods in Molecular Biology*; Humana Press Inc., 2018; Vol. 1852, pp. 221–237.
56. Rodríguez-Frómeta, R.A.; Gutiérrez, A.; Torres-Martínez, S.; Garre, V. Malic enzyme activity is not the only bottleneck for lipid accumulation in the oleaginous fungus Mucor circinelloides. *Appl. Microbiol. Biotechnol.* **2013**, *97*, 3063–3072, doi:10.1007/s00253-012-4432-2.
57. Valle-Maldonado, M.I.; Jácome-Galarza, I.E.; Gutiérrez-Corona, F.; Ramírez-Díaz, M.I.; Campos-García, J.; Meza-Carmen, V. Selection of reference genes for quantitative real time RT-PCR during dimorphism in the zygomycete Mucor circinelloides. *Mol. Biol. Rep.* **2015**, *42*, 705–711, doi:10.1007/s11033-014-3818-x.
58. Livak, K.J.; Schmittgen, T.D. Analysis of relative gene expression data using real-time quantitative PCR and. *Methods* **2001**, *25*, 402–408, doi:10.1006/meth.2001.1262.
59. Jia, G.; Fu, Y.; Zhao, X.; Dai, Q.; Zheng, G.; Yang, Y.; Yi, C.; Lindahl, T.; Pan, T.; Yang, Y.G.; et al. N6-Methyladenosine in nuclear RNA is a major substrate of the obesity-associated FTO. *Nat. Chem. Biol.* **2011**, *7*, 885–887, doi:10.1038/nchembio.687.
60. Trewick, S.C.; Henshaw, T.F.; Hausinger, R.P.; Lindahl, T.; Sedgwick, B. Oxidative demethylation by Escherichia coli AlkB directly reverts DNA base damage. *Nature* **2002**, *419*, 174–178, doi:10.1038/nature00908.
61. Falnes, P.; Johansen, R.F.; Seeberg, E. AlkB-mediated oxidative demethylation reverses DNA damage in Escherichia coli. *Nature* **2002**, *419*, 178–182, doi:10.1038/nature01048.
62. Velayos, A.; Eslava, A.P.; Iturriaga, E.A. A bifunctional enzyme with lycopene cyclase and phytoene synthase activities is encoded by the carRP gene of Mucor circinelloides. *Eur. J. Biochem.* **2000**, *267*, 5509–5519, doi:10.1046/J.1432-1327.2000.01612.X.
63. Yi, C.; He, C. DNA repair by reversal of DNA damage. *Cold Spring Harb. Perspect. Biol.* 2013, *5*, 12575–12576.
64. Kataoka, H.; Yamamoto, Y.; Sekiguchi, M. A new gene (alkB) of Escherichia coli that controls sensitivity to methyl methane sulfonate. *J. Bacteriol.* **1983**, *153*, 1301–1307, doi:10.1128/jb.153.3.1301-1307.1983.
65. Gauthier, G.; Klein, B.S. Insights into fungal morphogenesis and immune evasion. *Microbe* 2008, *3*, 416–423.
66. Pérez-Arques, C.; Navarro-Mendoza, M.I.; Murcia, L.; Lax, C.; Martínez-García, P.; Heitman, J.; Nicolás, F.E.; Garre, V. Mucor circinelloides thrives inside the phagosome through an Atf-mediated germination pathway. *MBio* **2019**, *10*, e02765-18, doi:10.1128/mBio.02765-18.